Proceedings of the ASME 2009 Fluids Engineering Division Summer Meeting
FEDSM2009
August 2-6, 2009, Vail, Colorado USA

FEDSM2009-78091

DNS/DPS OF INERTIAL DROPLET COALESCENCE IN HOMOGENEOUS ISOTROPIC TURBULENCE AND COMPARISON WITH PDF MODEL PREDICTIONS USING THE DIRECT QUADRATURE METHOD OF MOMENTS

Dirk Wunsch[1,2], **Roel Belt**[1,2], **Pascal Fede**[1,2], **Olivier Simonin**[1,2*]
[1] Université de Toulouse; INPT, UPS; IMFT
31400 Toulouse, France

[2] CNRS, Institut de Mécanique des Fluides de Toulouse
31400 Toulouse, France
Email: simonin@imft.fr

ABSTRACT

To analyze in detail the coalescence mechanisms and validate modeling approaches, deterministic Lagrangian simulations of droplet trajectories (DPS) coupled with Direct Numerical Simulations (DNS) of a Homogeneous Isotropic Turbulence (HIT) are performed. The influence of the colliding particle velocity correlations induced by the fluid turbulence on the rate of droplet coalescence is investigated for different particle inertia. The results are compared to predictions using the Direct Quadrature Method of Moments (DQMOM) accounting for coalescence. The particle diameter distribution is written as a summation of Dirac functions. This allows to derive Eulerian transport equations for the dispersed phase statistics, which account for coalescence and conserve the low-order moments of the particle size distribution. The collision terms are modeled applying the molecular chaos assumption in order to account for coalescence. Particle size distributions and moments obtained from DQMOM are compared to those of the DNS/DPS simulations in function of particle inertia.

INTRODUCTION

The study of collisions between particles in turbulent dispersed multiphase flows is of interest for many engineering applications. Examples of flows where droplet coalescence is likely to play an important role include many topics such as solid-fuel rocket propulsion, internal combustion engines and electric power generation by liquid fuel turbines. The droplet size generally has a major influence on the global performance of the system and must be accurately taken into account in numerical simulations. As the carrier flow is often turbulent, droplets located in the vicinity of the same point may have different velocities, collide and perhaps coalesce leading to a strong modification of the droplet size distribution.

The statistical representation of the coalescence rates is gained based on a Lagrangian tracking of the dispersed phase, here referred to as Discrete Particle Simulation (DPS), in a physical study of coalescence in Homogeneous Isotropic Turbulence. This approach is coupled with Direct Numerical Simulations (DNS) in order to account for the influence of the turbulent motion of a fluid on the particle distribution. Coalescence is accounted for using an algorithm allowing to detect collision in a broad droplet size distribution. This algorithm was validated for dry granular test cases [1]. The results are compared to predictions using the Direct Quadrature Method of Moments (DQMOM) accounting for coalescence. The here applied DQMOM approach [2] is a recently developed extension of the approach by Marchisio and Fox [3] based on the formalism of the joint fluid-particle PDF approach by Simonin [4].

Coalescence phenomena are various and each collision between two droplets leads to the creation of one to several new droplets, depending on the relative properties of the colliding droplets. Several studies concerned with coalescence phenomena have been performed, pointing out the diversity of the collision outcome [5–7]. In this study, in order to better understand

*Address all correspondence to this author.

the physical mechanisms of turbulence-coalescence interaction, only the permanent coalescence regime is considered. Each collision leads to permanent coalescence.

The article is structured as follows. First, the DNS/DPS approach is explained. Second, the DQMOM approach is detailed by explaining the general formalism, the closure of the collision operator and then outlining the equations solved in the frame of this work. Then the fluid flow is described and finally results are presented for the comparison of DQMOM with DNS/DPS.

DNS/DPS APPROACH

Direct Numerical Simulations (DNS) coupled with a Lagrangian tracking of the particle phase (DPS) are performed here and have been extensively used to investigate gas-particle flows [8–11]. The flow configuration is a Homogeneous Isotropic Turbulence (HIT) forced by a scheme initially proposed by Eswaran and Pope [12], which assures a statistical steadiness. The particles are considered as rigid spheres with diameters smaller than the Kolmogorov turbulence length scale η_K. The turbulence modulation by the dispersed phase (two-way coupling) is not considered, as the particle mass fraction is small. Assuming that the particle fluid density ratio ($\rho_p \gg \rho_f$) is large, the forces acting on the particle are reduced to the drag force only. Thus, the governing equations of the N_p particle system in interaction with the surrounding flow field and undergoing particle-particle collisions are written as

$$\begin{aligned} \frac{d\mathbf{x}_p}{dt} &= \mathbf{v}_p \\ m_p \frac{d\mathbf{v}_p}{dt} &= m_p \frac{[\mathbf{v}_p - \mathbf{u}_{f@p}]}{\tau_p} + \sum_{i=1;j\neq i}^{N_p} \mathbf{F}_{p,ij} \end{aligned} \tag{1}$$

where $\mathbf{x}_p, \mathbf{u}_p$ are the position and velocity vectors of the particle p and m_p is the particle mass. $\mathbf{u}_{f@p}$ is the undisturbed fluid velocity at the position of the particle and $\mathbf{F}_{p,ij}$ represents the impulsive force resulting from particle-particle collisions. As two-way coupling is neglected, $\mathbf{u}_{f@p}$ is computed with an accurate interpolation scheme [13]. The particle response time τ_p is given using the relation of Schiller and Naumann [14] by

$$\begin{aligned} \tau_p &= \frac{4}{3}\frac{\rho_p}{\rho_f}\frac{d_p}{C_D}\frac{1}{|\mathbf{v}_p - \mathbf{u}_{f@p}|} \\ C_D &= \frac{24}{Re_p}\left(1 + 0.15 Re_p^{0.687}\right) \\ Re_p &= \frac{|\mathbf{v}_p - \mathbf{u}_{f@p}|\, d_p}{\nu_f} \end{aligned} \tag{2}$$

with d_p the particle diameter and ν_f the kinematic viscosity of the fluid. Coalescence is modeled assuming that each collision leads to permanent coalescence. Other collision outcomes as identified by several authors [5–7] are not regarded for the sake distinctness. The mass and momentum conservation equations of two particles undergoing coalescence are written as

$$\begin{aligned} m^* &= m_p + m_q \\ m^*\mathbf{v}^* &= m_p\mathbf{v}_p + m_q\mathbf{v}_q \end{aligned} \tag{3}$$

with m_p and m_q the mass of the particles before coalescence and m^* after. Analogous for the particle velocities $\mathbf{v}_p, \mathbf{v}_q$ and $\mathbf{v}^*$. The corresponding particle diameter is directly deductible from the mass conservation equations as the particle density is constant and the particles are modeled as rigid spheres, as mentioned above. The position of the new particle that arises from coalescence is given as

$$\mathbf{x}^* = \frac{d_p^3\mathbf{x}_p + d_q^3\mathbf{x}_q}{d^{*3}} \tag{4}$$

with $\mathbf{x}^*$ the position of the new particle and d_p, d_q and d^* the particle diameters. Coalescence is detected using a recently developed algorithm allowing detecting collisions in a poly-dispersed particle mixture [1].

DQMOM APPROACH

The here used DQMOM approach is an extension of the approach proposed by Marchisio and Fox [3] based on the formalism of the joint fluid-particle PDF approach by Simonin [4] recently developed by Belt and Simonin [2].

To account for droplet coalescence (particle aggregation) or poly-dispersion in the frame of the Euler-Euler modeling approach is challenging. Marchisio and Fox [3] proposed the DQMOM approach to tackle these difficulties. However, as the velocity distribution for a given diameter is represented by a Dirac, coalescence effects appear only in the mass balance equations. Consequently, as outlined by Belt and Simonin [2], particle momentum and particle kinetic stress transport equations cannot be written accounting for coalescence effects. Instead, in the approach of Marchisio and Fox [3], an ad-hoc formulation of the multi-class Eulerian approach without collision modeling is applied. In the novel approach, these equations can be derived accounting for particle coalescence. This new approach is briefly summarized in the following. The reader may refer to [2] for a more complete description of the formalism.

General DQMOM formalism

The dispersed phase statistics can be described in turbulent two-phase flows in terms of the joint fluid-particle probability

density function (pdf) $f_{fp}(\mathbf{x},t,\mathbf{c}_f,\mu_p,\mathbf{c}_p)$, which is defined such that $f_{fp}(\mathbf{x},t,\mathbf{c}_f,\mu_p,\mathbf{c}_p)d\mathbf{c}_f d\mu_p d\mathbf{c}_p d\mathbf{x}$ is the probable number of droplets at time t with the center of mass located in the volume $[\mathbf{x},\mathbf{x}+d\mathbf{x}]$, a translation velocity $\mathbf{u}_p$ in $[\mathbf{c}_p,\mathbf{c}_p+d\mathbf{c}_p]$ and a mass m_p in $[\mu_p,\mu_p+d\mu_p]$, seeing a locally undisturbed fluid velocity $\mathbf{u}_{f@p}$ in $[\mathbf{c}_f,\mathbf{c}_f+d\mathbf{c}_f]$. The evolution equation can be written as a Boltzmann-type equation [4]:

$$\begin{aligned}\frac{\partial f_{fp}}{\partial t}+\frac{\partial}{\partial x_j}\left(c_{p,j}f_{fp}\right)+\frac{\partial}{\partial c_{p,j}}\left(\langle\frac{\mathrm{d}u_{p,j}}{\mathrm{d}t}|\mu_p,\mathbf{c}_p,\mathbf{c}_f\rangle f_{fp}\right)\\+\frac{\partial}{\partial c_{f,j}}\left(\langle\frac{\mathrm{d}u_{f@p,j}}{\mathrm{d}t}|\mu_p,\mathbf{c}_p,\mathbf{c}_f\rangle f_{fp}\right)\\+\frac{\partial}{\partial \mu_p}\left(\langle\frac{\mathrm{d}m_p}{\mathrm{d}t}|\mu_p,\mathbf{c}_p,\mathbf{c}_f\rangle f_{fp}\right)\\=\left(\frac{\partial f_{fp}}{\partial t}\right)_{coll}\end{aligned}\tag{5}$$

where $\langle.\rangle$ represents an ensemble averaging operator and $\frac{d}{dt}$ the rate of change along the particle path of any particle property. The notation $\langle.|\mu_p,\mathbf{c}_p,\mathbf{c}_f\rangle$ is written for the conditional expectation $\langle.|m_p=\mu_p,\mathbf{u}_p=\mathbf{c}_p,\mathbf{u}_{f@p}=\mathbf{c}_f\rangle$. Exact expressions for the third to fifth term can be found in [4]. The collision operator $\left(\frac{\partial f_{fp}}{\partial t}\right)_{coll}$ will be detailed below.

Marchisio and Fox [3] wrote the particle pdf f_p as a summation of N Dirac functions in mass and velocity space:

$$\begin{aligned}f_p(\mathbf{x},t,\mu_p,\mathbf{c}_p)=\\\sum_{\alpha=1}^{N}\omega_\alpha(\mathbf{x},t)\delta(\mu_p-\tilde{\mu}_{p,\alpha}(\mathbf{x},t))\delta(\mathbf{c}_p-\tilde{\mathbf{c}}_{p,\alpha}(\mathbf{x},t))\end{aligned}\tag{6}$$

where $\mu_{p,\alpha}(\mathbf{x},t)$ and $\mathbf{c}_{p,\alpha}(\mathbf{x},t)$ are the mass and velocity of class α, respectively. As seen in (6), one single mean velocity is associated with each mass and as a consequence transport equations for the particle agitation cannot be derived. Belt and Simonin [2] define for each class one mass associated with a velocity distribution, which is written as:

$$f_{fp}(\mathbf{x},t,\mu_p,\mathbf{c}_p,\mathbf{c}_f)=n_p(\mathbf{x},t)h^*_{fp}(\mathbf{x},t,\mathbf{c}_p,\mathbf{c}_f|\mu_p)g^*(\mathbf{x},t,\mu_p)\tag{7}$$

with $n_p(\mathbf{x},t)$ the number of particles per unit volume at $\mathbf{x}$ and t. $h^*_{fp}(\mathbf{x},t,\mathbf{c}_p,\mathbf{c}_f|\mu_p)$ is the joint fluid-particle velocity probability density function at time t, conditioned by the mass m_p equal to μ_p, with the center of mass located in the volume $[\mathbf{x},\mathbf{x}+d\mathbf{x}]$ and a translation velocity $\mathbf{u}_p$ in $[\mathbf{c}_p,\mathbf{c}_p+d\mathbf{c}_p]$, seeing a locally undisturbed fluid velocity $\mathbf{u}_{f@p}$ in $[\mathbf{c}_f,\mathbf{c}_f+d\mathbf{c}_f]$. $g^*(\mathbf{x},t,\mu_p)$ is the mass probability density function at time t with the center of mass located in the volume $[\mathbf{x},\mathbf{x}+d\mathbf{x}]$ and a mass m_p in $[\mu_p,\mu_p+d\mu_p]$. The pdfs h^*_{fp} and g^* verify:

$$\int h^*_{fp}(\mathbf{x},t,\mathbf{c}_p,\mathbf{c}_f|\mu_p)\mathrm{d}\mathbf{c}_p\mathrm{d}\mathbf{c}_f=1\quad\forall\,\mu_p\tag{8}$$

$$\int g^*(\mathbf{x},t,\mu_p)\mathrm{d}\mu_p=1\tag{9}$$

Belt and Simonin [2] write the pdf g^*, similar to [3], as a summation of Dirac functions with the sum of the weights ω_α over all classes equal to one (10).

$$g^*(\mathbf{x},t,\mu_p)=\sum_{\alpha=1}^{N}\omega_\alpha(\mathbf{x},t)\delta(\mu_p-\tilde{\mu}_{p,\alpha}(\mathbf{x},t))\tag{10}$$

This presumed pdf g^* is equivalent to make the Gauss quadrature approximation for the moments of g^*:

$$\int\mu_p^k g^*(x,t,\mu_p)\mathrm{d}\mu_p=\sum_{\alpha=1}^{N}\tilde{\mu}^k_{p,\alpha}(\mathbf{x},t)\omega_\alpha(\mathbf{x},t)\tag{11}$$

The weights ω_α and the abscissas $\tilde{\mu}_{p,\alpha}$ in (10) are unknown, thus $2N$ unknowns must be determined. With the help of the Gauss quadrature approximation, the moments of g^* can be computed. Following the DQMOM approach $2N$ transport equations on the low-order mass-moments are derived by integration of the Boltzmann-type equation (5) multiplied with μ_p^k. After some manipulation the following system is obtained with k ranging from 0 to $2N-1$:

$$\begin{aligned}&\int\mu_p^k\left(\frac{\partial f_{fp}}{\partial t}\right)_{coll}\mathrm{d}\mathbf{c}_p\mathrm{d}\mathbf{c}_f\mathrm{d}\mu_p\\&=(1-k)\sum_{\alpha=1}^{N}\tilde{\mu}^k_{p,\alpha}\left[\frac{\partial}{\partial t}(n_\alpha)+\frac{\partial}{\partial x_j}\left(\langle c_{p,j}\rangle_\alpha n_\alpha\right)\right]\\&\quad+k\sum_{\alpha=1}^{N}\tilde{\mu}^{k-1}_{p,\alpha}\left[\frac{\partial}{\partial t}(n_\alpha\tilde{\mu}_{p,\alpha})+\frac{\partial}{\partial x_j}\left(\langle c_{p,j}\rangle_\alpha n_\alpha\tilde{\mu}_{p,\alpha}\right)-n_\alpha\langle\Gamma\rangle_\alpha\right]\end{aligned}\tag{12}$$

For the sake of clarity, the quantity dependencies with respect to $\mathbf{x}$ and t are not written out in (12). The mean number of particles per unit volume n_α with mass $\tilde{\mu}_{p,\alpha}$ is defined as $n_\alpha=\omega_\alpha n$. The physical meaning of the weight ω_α appears in this approach, as the ratio of number of droplets per class α to the total number of droplets at $\mathbf{x}$ and t. System (12) gives the values for the N abscissas $\tilde{\mu}_{p,\alpha}$ and N weights n_α, from which the droplet diameter distribution is reconstructed. This reconstructed distribution should show the correct moments up to the order $2N-1$. The operator $\langle\phi\rangle_\alpha$ represents the conditional average on a mass m_p

equal to $\tilde{\mu}_{p,\alpha}$: $\langle\phi\rangle_\alpha = \int \phi h^*_{fp}(\mathbf{x},t,\mathbf{c}_p,\mathbf{c}_f|\tilde{\mu}_{p,\alpha})\mathrm{d}\mathbf{c}_p\mathrm{d}\mathbf{c}_f$. The term $n_\alpha\langle\Gamma\rangle_\alpha$ represents the evaporation rate of droplets, which is zero throughout this work.

For $N=1$ the equation (12) is identical to the number $(k=0)$ and mass $(k=1)$ transport equations for monodisperse droplets derived by Simonin [4]. Also, (12) is equivalent to the system obtained by Marchisio and Fox [3] if written in terms of diameter. However, system (12) is not closed since it contains the velocity $\langle\mathbf{c}_p\rangle_\alpha$ conditioned by the mass of class α. Following a similar way as Simonin [4] to derive transport equations for momentum, particle kinetic stress and fluid-particle covariance, the velocity $\langle\mathbf{c}_p\rangle_\alpha$ can be obtained in the framework of the DQMOM approach. Those equations are in agreement with Simonin's [4] transport equations for a monodisperse droplet cloud. For more details, the reader may refer to [2] and [4], readers interested in the resolution of the equation system to [2] and [3].

In a Homogeneous Isotropic Turbulence, as in this study, all variations with respect to $\frac{\partial}{\partial x_j}$ are zero and thus equation (12) simplifies significantly. In particular the momentum balance equation does not need to be solved, since the mean velocity is equal to zero. As detailed below, the particle kinetic energy is required for the closure of the collision term. In a first step, within this work, the corresponding values of q_p^2 are directly obtained from the performed DNS/DPS simulations. In a second step, the particle kinetic stress tensor equation is solved in the DQMOM approach. In order to account for the interaction of the particle phase with the fluid turbulent motion, the mean particle response time $\tau^F_{fp} = \langle\tau_p\rangle_\alpha$ and the fluid-particle symmetrical velocity covariance tensor $R_{fp,\gamma\beta} = \frac{1}{2}\left(\langle u'_{f@p,\gamma}c'_{p,\beta}\rangle_\alpha + \langle c'_{p,\gamma}u'_{f@p,\beta}\rangle_\alpha\right)$ are then needed. The value for τ^F_{fp} is taken from the DNS/DPS simulations. A transport equation for R_{fp} can be derived in the DQMOM framework (14). The equilibrium state from the theory of Tchen and Hinze [15] is used to determine the fluid-particle covariance, which is given using the relation of Tchen [15] $q_{fp} = \frac{2q_f}{1+St}$ where the Stokes number is defined as $St = \frac{\tau^F_{fp}}{T_L}$, when the particle kinetic stress equation is solved only. The particle kinetic stress tensor equation is given in (13).

$$
\begin{aligned}
&\int c'_{p,\gamma}c'_{p,\beta}\mu_p^k\left(\frac{\partial f_{fp}}{\partial t}\right)_{coll}\mathrm{d}\mathbf{c}_p\mathrm{d}\mathbf{c}_f\mathrm{d}\mu_p + E \\
&= (1-k)\sum_{\alpha=1}^{N}\tilde{\mu}^k_{p,\alpha}\left[\frac{\partial}{\partial t}\left(n_\alpha\langle c'_{p,\gamma}c'_{p,\beta}\rangle_\alpha\right)\right. \\
&\quad + \frac{\partial}{\partial x_j}\left(n_\alpha\langle c'_{p,\gamma}c'_{p,\beta}\rangle_\alpha\langle c_{p,j}\rangle_\alpha\right) + \frac{\partial}{\partial x_j}\left(n_\alpha\langle c'_{p,\gamma}c'_{p,\beta}c'_{p,j}\rangle_\alpha\right) \\
&\quad + n_\alpha\langle c'_{p,\gamma}c'_{p,j}\rangle_\alpha\frac{\partial}{\partial x_j}\langle c_{p,\beta}\rangle_\alpha + n_\alpha\langle c'_{p,\beta}c'_{p,j}\rangle_\alpha\frac{\partial}{\partial x_j}\langle c_{p,\gamma}\rangle_\alpha \\
&\qquad\left. -n_\alpha\langle c'_{p,\beta}\frac{F'_\gamma}{m}\rangle_\alpha - n_\alpha\langle c'_{p,\gamma}\frac{F'_\beta}{m}\rangle_\alpha\right] \\
&+k\sum_{\alpha=1}^{N}\tilde{\mu}^{k-1}_{p,\alpha}\left[\frac{\partial}{\partial t}\left(n_\alpha\tilde{\mu}_{p,\alpha}\langle c'_{p,\gamma}c'_{p,\beta}\rangle_\alpha\right)\right. \\
&+ \frac{\partial}{\partial x_j}\left(n_\alpha\tilde{\mu}_{p,\alpha}\langle c'_{p,\gamma}c'_{p,\beta}\rangle_\alpha\langle c_{p,j}\rangle_\alpha\right) + \frac{\partial}{\partial x_j}\left(n_\alpha\tilde{\mu}_{p,\alpha}\langle c'_{p,\gamma}c'_{p,\beta}c'_{p,j}\rangle_\alpha\right) \\
&\quad + n_\alpha\tilde{\mu}_{p,\alpha}\langle c'_{p,\gamma}c'_{p,j}\rangle_\alpha\frac{\partial}{\partial x_j}\langle c_{p,\beta}\rangle_\alpha + n_\alpha\tilde{\mu}_{p,\alpha}\langle c'_{p,\beta}c'_{p,j}\rangle_\alpha\frac{\partial}{\partial x_j}\langle c_{p,\gamma}\rangle_\alpha \\
&\quad - n_\alpha\tilde{\mu}_{p,\alpha}\langle c'_{p,\beta}\frac{F'_\gamma}{m}\rangle_\alpha - n_\alpha\tilde{\mu}_{p,\alpha}\langle c'_{p,\gamma}\frac{F'_\beta}{m}\rangle_\alpha \\
&\quad \left. - n_\alpha\langle\Gamma c'_{p,\gamma}c'_{p,\beta}\rangle_\alpha\right] \qquad (13)
\end{aligned}
$$

The only term of equation (13) that remains in the equation for a Homogeneous Isotropic Turbulence are detailed below.

Finally, the fluid-particle covariance equation (14) is solved. τ^F_{fp} is taken again from the DNS/DPS simulations and the fluid energy q_f^2 is also known. The fluid-particle covariance equation writes as:

$$
\begin{aligned}
&\mathcal{C}(c'_{f,\beta}c'_{p,\gamma}\mu_p^k) + E' = \\
&\qquad (1-k)\sum_{\alpha=1}^{N}\tilde{\mu}^k_{p,\alpha}e_\alpha + k\sum_{\alpha=1}^{N}\tilde{\mu}^{k-1}_{p,\alpha}f_\alpha \qquad (14)
\end{aligned}
$$

where e_α and f_α are the source terms of the following equations:

$$
\begin{aligned}
&\frac{\partial}{\partial t}\left(n_\alpha\langle c'_{f,\beta}c'_{p,\gamma}\rangle_\alpha\right) + \frac{\partial}{\partial x_j}\left(n_\alpha\langle c'_{f,\beta}c'_{p,\gamma}\rangle_\alpha\langle c_{p,j}\rangle_\alpha\right) \\
&\quad + \frac{\partial}{\partial x_j}\left(n_\alpha\langle c'_{f,\beta}c'_{p,\gamma}c'_{p,j}\rangle_\alpha\right) \\
&\quad - n_\alpha\langle c'_{f,\beta}\frac{F'_\gamma}{m_p}\rangle_\alpha - n_\alpha\langle c'_{p,\gamma}A_\beta\rangle_\alpha \quad = \quad e_\alpha \qquad (15) \\
&\frac{\partial}{\partial t}\left(n_\alpha\tilde{\mu}_{p,\alpha}\langle c'_{f,\beta}c'_{p,\gamma}\rangle_\alpha\right) + \frac{\partial}{\partial x_j}\left(n_\alpha\tilde{\mu}_{p,\alpha}\langle c'_{f,\beta}c'_{p,\gamma}\rangle_\alpha\langle c_{p,j}\rangle_\alpha\right) \\
&\quad + \frac{\partial}{\partial x_j}\left(n_\alpha\tilde{\mu}_{p,\alpha}\langle c'_{f,\beta}c'_{p,\gamma}c'_{p,j}\rangle_\alpha\right) \\
&\quad - n_\alpha\tilde{\mu}_{p,\alpha}\langle c'_{f,\beta}\frac{F'_\gamma}{m_p}\rangle_\alpha - n_\alpha\tilde{\mu}_{p,\alpha}\langle c'_{p,\gamma}A_\beta\rangle_\alpha \\
&\quad - n_\alpha\langle\Gamma c'_{f,\beta}c'_{p,\gamma}\rangle_\alpha \quad = \quad f_\alpha \qquad (16)
\end{aligned}
$$

The remaining terms in the equation are explained below when detailed for Homogeneous Isotropic Turbulence. The reader may note that the term E and E' on the left hand side of equations (13) and (14) is equal to zero in a Homogeneous Isotropic Turbulence. For its definition as well as an exhaustive explanation of the terms in (13) and (14) the reader may refer to [2].

Closure of collision operator

The coalescence operator $\mathcal{C}(\psi)$ is the integral of the change in a quantity ψ (for a distinct collision) multiplied with its probable collision frequency over all binary collisions. If ψ^* is the quantity after collision and ψ before collision, the change in ψ can be written as $\Delta\psi = \psi^* - \psi$ and thus the coalescence operator $\mathcal{C}(\psi)$ for two particles P and Q as:

$$\mathcal{C}(\Psi) = \frac{1}{2} d_{pq}^2 \int_{\mathbf{w}\cdot\mathbf{k}<0} (\Psi_{pq}^* - \Psi_{pq}) \, [\mathbf{w}\cdot\mathbf{k}] \\ f_{fp}^{(2)}(\mathbf{c}_{f@p}, \mu_p, \mathbf{c}_p, \mathbf{x}, \mathbf{c}_{f@q}, \mu_q, \mathbf{c}_q, \mathbf{x} + d_{pq}\mathbf{k}, t) \\ \mathrm{d}\mathbf{k}\mathrm{d}\mu_p\mathrm{d}\mu_q\mathrm{d}\mathbf{c}_{f@p}\mathrm{d}\mathbf{c}_p\mathrm{d}\mathbf{c}_{f@q}\mathrm{d}\mathbf{c}_q \tag{17}$$

where $d_{pq} = (d_p + d_q)/2$ is the collision diameter, $\mathbf{w} = \mathbf{c}_q - \mathbf{c}_p$ is the relative velocity between the two colliding droplets, $\mathbf{k}$ is the unit center connecting vector pointing from particle P to Q. $f_{fp}^{(2)}(\mathbf{c}_{f@p}, \mu_p, \mathbf{c}_p, \mathbf{x}_p, \mathbf{c}_{f@q}, \mathbf{c}_q, \mu_q, \mathbf{x}_q, t)$ is the joint fluid-particle-fluid-particle pair distribution function. The particle pair distribution function $f_p^{(2)}$ is per definition obtained by integration over the particle velocities as given in equation (18).

$$f_p^{(2)}(\mathbf{c}_p, \mu_p, \mathbf{x}, \mu_q, \mathbf{c}_q, \mathbf{x} + d_{pq}\mathbf{k}, t) \\ = \int\int f_{fp}^{(2)}(\mathbf{c}_{f@p}, \mu_p, \mathbf{c}_p, \mathbf{x}, \mathbf{c}_{f@q}, \mu_q, \mathbf{c}_q, \mathbf{x} + d_{pq}\mathbf{k}, t) \\ \mathrm{d}\mathbf{c}_{f@p}\mathrm{d}\mathbf{c}_{f@q} \tag{18}$$

According to the "molecular chaos" assumption the particle pair distribution function $f_p^{(2)}$ can be written as a product of to single one-particle distribution functions:

$$f_p^{(2)}(\mathbf{c}_p, \mu_p, \mathbf{x}, \mu_q, \mathbf{c}_q, \mathbf{x} + d_{pq}\mathbf{k}, t) \\ \approx f_p(\mathbf{c}_p, \mu_p, \mathbf{x}, t) \, f_p(\mathbf{c}_q, \mu_q, \mathbf{x} + d_{pq}\mathbf{k}, t), \tag{19}$$

It needs to be mentioned that according to [9] the "molecular chaos" assumption is valid only, if the particle response time is much larger than the fluid Lagrangian time scale. If the particle response time is of the same order or smaller than the fluid Lagrangian time scale, the particle velocities become correlated through the interaction with the fluid. This can be accounted for by a specific closure of $f_{fp}^{(2)}$ proposed by [9]. Nevertheless, the "molecular chaos" assumption is the simplest approach and is used here.

The coalescence operator is here written, similar to [3] as outlined in [2], as a function of the "birth" rate $\mathcal{B}$ and "death" rate $\mathcal{D}$ for a quantity $\psi = \mu_p^k$:

$$\mathcal{C}(\Psi) = \mathcal{B}(\Psi) - \mathcal{D}(\Psi) \tag{20}$$

$$\mathcal{B}(\Psi) = \frac{1}{2} \int \Psi_{pq}^* \, \beta(\mu_p, \mu_q) \\ g^*(\mathbf{x}, t, \mu_p) g^*(\mathbf{x}, t, \mu_q) \mathrm{d}\mu_p \mathrm{d}\mu_q \tag{21}$$

$$\mathcal{D}(\Psi) = \int \Psi_p \, \beta(\mu_p, \mathbf{c}_p, \mu_q, \mathbf{c}_q) \\ g^*(\mathbf{x}, t, \mu_p) g^*(\mathbf{x}, t, \mu_q) \mathrm{d}\mu_p \mathrm{d}\mu_q \tag{22}$$

with $\beta(\mu_p, \mu_q)$ the radial relative velocity. It can be written as:

$$\beta = \pi n_p^2 d_{pq}^2 \left(\frac{16}{\pi} \frac{1}{3} (q_p^2 + q_q^2) \right)^{1/2} \tag{23}$$

DQMOM in Homogeneous Isotropic Turbulence (HIT)

The DQMOM approach is here compared with a homogeneous isotropic turbulence coupled with a dispersed phase of spherical particles undergoing coalescence. As mentioned above, all variations with respect to $\frac{\partial}{\partial x_j}$ are zero and equation (12) and (13) simplify significantly. Five different cases are regarded here. In the first case i) only the number and mass balance equation are solved. The particle kinetic energy is extracted from the DNS/DPS simulations. Second, the particle kinetic stress equation is in case ii) solved making use of from DNS/DPS values for the mean particle response time, while the fluid particle covariance is modeled following the theory of Tchen and Hinze [15]. In case iii) additionally the fluid particle covariance equation is solved, with the fluid energy from the DNS/DPS simulations. In case iv) a collision term in the particle kinetic stress equation is added. And last in case v) dry granular simulations are performed in order to evaluate the influence of the collision term in the particle kinetic stress equation. The equations to solve are the following. For the number and mass balance equation (12) the source terms can be written per class α:

i) Number and mass balance equation HIT

$$\frac{\partial}{\partial t}(n_\alpha) = a_\alpha \tag{24}$$

$$\frac{\partial}{\partial t}(n_\alpha \tilde{\mu}_{p,\alpha}) = b_\alpha \tag{25}$$

Then, the system to solve becomes (12), with k ranging from 0 to $2N-1$:

$$(1-k) \sum_{\alpha=1}^{N} \tilde{\mu}_{p,\alpha}^k a_\alpha + k \sum_{\alpha=1}^{N} \tilde{\mu}_{p,\alpha}^{k-1} b_\alpha = \mathcal{C}(\mu_p^k) \tag{26}$$

where $\mathcal{C}(\mu_p^k)$ represents the collision term as defined in (20).

ii) Particle kinetic stress equation (HIT) The particle kinetic stress equation can be written as seen in (28). It can also be obtained from (27). As the particle number and mass are known from (26), (27) contains the same information as (28) as it is only weighted by a different factor. The source terms are related and c_α can be expressed in terms of a_α, b_α and d_α.

$$\frac{\partial}{\partial t}\left(n_\alpha\langle c'_{p,\gamma}c'_{p,\beta}\rangle_\alpha\right) - n_\alpha\langle c'_{p,\beta}\frac{F'_\gamma}{m}\rangle_\alpha - n_\alpha\langle c'_{p,\gamma}\frac{F'_\beta}{m}\rangle_\alpha = c_\alpha \quad (27)$$

$$\frac{\partial}{\partial t}\left(n_\alpha\tilde{\mu}_{p,\alpha}\langle c'_{p,\gamma}c'_{p,\beta}\rangle_\alpha\right) - n_\alpha\tilde{\mu}_{p,\alpha}\langle c'_{p,\beta}\frac{F'_\gamma}{m}\rangle_\alpha - n_\alpha\tilde{\mu}_{p,\alpha}\langle c'_{p,\gamma}\frac{F'_\beta}{m}\rangle_\alpha = d_\alpha \quad (28)$$

(13) can be written as shown in (29), if the influence of coalescence is not accounted for in the particle kinetic stress equation. In the case $ii)$ the system to solve consists thus of (26) and (29). This assumption is valid only, if the effect of collisions on particle kinetic stress is less important than the interaction with the fluid. In this case the source terms $c_\alpha = 0$ and $d_\alpha = 0$ equal zero.

$$(1-k)\sum_{\alpha=1}^{N}\tilde{\mu}^k_{p,\alpha}c_\alpha + k\sum_{\alpha=1}^{N}\tilde{\mu}^{k-1}_{p,\alpha}d_\alpha = \mathcal{C}\left(\mu^k_p c'_{p,\beta}c'_{p,\gamma}\right) = 0 \quad (29)$$

The interaction with the fluid turbulent motion is expressed by the force terms F' in (28). They are written following [4] as follows:

$$n_\alpha\tilde{\mu}_{p,\alpha}\langle c'_{p,\beta}\frac{F'_\gamma}{m}\rangle_\alpha - n_\alpha\tilde{\mu}_{p,\alpha}\langle c'_{p,\gamma}\frac{F'_\beta}{m}\rangle_\alpha \approx -n_\alpha\tilde{\mu}_{p,\alpha}\frac{2}{\tau^F_{fp,\alpha}}\left[\langle c'_{p,\gamma}c'_{p,\beta}\rangle_\alpha - R_{fp,\gamma\beta}\right] \quad (30)$$

Where the fluid-particle covariance tensor $R_{fp,\gamma\beta}$ is modeled using $q_{fp} = \frac{2q_f}{1+St}$. The mean particle response time $\tau^F_{fp,\alpha}$ is extracted from the DNS/DPS simulations.

iii) Fluid particle covariance equation (HIT) The fluid particle covariance equation is given in the case of a Homogeneous Isotropic Turbulence by (31).

$$\frac{\partial}{\partial t}\left(n_\alpha\tilde{\mu}_{p,\alpha}\langle c'_{f,\beta}c'_{p,\gamma}\rangle_\alpha\right) - n_\alpha\tilde{\mu}_{p,\alpha}\langle c'_{f,\beta}\frac{F'_\gamma}{m_p}\rangle_\alpha - n_\alpha\tilde{\mu}_{p,\alpha}\langle c'_{p,\gamma}A_\beta\rangle_\alpha = f_\alpha \quad (31)$$

The force terms can be written as:

$$n_\alpha\tilde{\mu}_{p,\alpha}\langle c'_{f,\beta}\frac{F'_\gamma}{m_p}\rangle_\alpha - n_\alpha\tilde{\mu}_{p,\alpha}\langle c'_{p,\gamma}A_\beta\rangle_\alpha \approx -n_\alpha\tilde{\mu}_{p,\alpha}\frac{2}{\tau^F_{fp,\alpha}}\left[\langle c'_{f,\gamma}c'_{p,\beta}\rangle_\alpha - \langle c'_{f,\gamma}c'_{f,\beta}\rangle_\alpha\right] - n_\alpha\tilde{\mu}_{p,\alpha}\frac{1}{T_L}\langle c'_{f,\gamma}c'_{p,\beta}\rangle_\alpha \quad (32)$$

iv) Collision term in particle kinetic stress equation In general it is difficult to write the collision term $\int q_p^2\mu_p^k\left(\frac{\partial f_{fp}}{\partial t}\right)_{coll}\mathrm{d}\mathbf{c}_p\mathrm{d}\mathbf{c}_f\mathrm{d}\mu_p$ in (13). In the here presented case, a Homogeneous Isotropic Turbulence, the particle mean velocity is zero, as already mentioned. This allows to write the coalescence term making use of (3) and applying (20) and with $\psi = \mu_p^k q_p^2$, if f_p is assumed Gaussian, as it is justified in this isotropic flow configuration. In a first attempt we can then write with $\Lambda = 1$:

$$\mathcal{B}\left(\mu_p^k q_p^2\right) = \Lambda\,\frac{1}{2}\sum_\alpha\sum_\kappa\beta_{\alpha,\kappa}\,\mu_p^{k,*}\,\frac{3}{2}\left(\frac{\mu_{p,\alpha}\left(\frac{2}{3}q^2_{p,\alpha}\right)^{\frac{1}{2}} + \mu_{p,\kappa}\left(\frac{2}{3}q^2_{p,\kappa}\right)^{\frac{1}{2}}}{\mu_{p,\alpha}+\mu_{p,\kappa}}\right)^2 \quad (33)$$

$$\mathcal{D}\left(\mu_p^k q_p^2\right) = \Lambda\sum_\alpha\sum_\kappa\beta_{\alpha,\kappa}\,\mu^k_{p,\alpha}\,\frac{2}{3}\,q^2_{p,\alpha} \quad (34)$$

The equations to solve are then (26) and (35):

$$(1-k)\sum_{\alpha=1}^{N}\tilde{\mu}^k_{p,\alpha}c_\alpha + k\sum_{\alpha=1}^{N}\tilde{\mu}^{k-1}_{p,\alpha}d_\alpha = \mathcal{C}\left(\mu^k_p q^2_p\right) \quad (35)$$

The term E in (13) equals zero in a Homogeneous Isotropic Turbulence, as mentioned above. For further information, the reader may refer to [2].

v) Influence of Collision terms in dry granular flows In this last case the influence of the collision term in the particle kinetic stress equation is evaluated. Dry granular simulations are therefore compared with DQMOM predictions for three different dry granular cases. In the first one, the number and mass balance equation only are solved and the particle kinetic energy is updated using results from DNS/DPS simulations. In the second dry granular case, the particle kinetic stress equation is solved, while the collision term is neglected and finally this collision term is taken into consideration in the last dry granular case. The collision term is shown under iv).

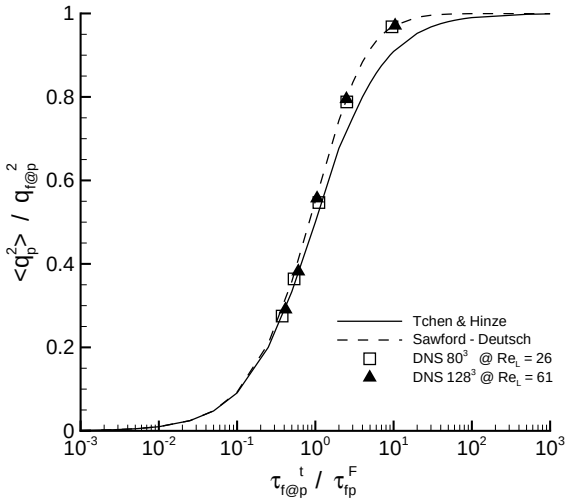

Figure 1. Simulated cases in comparison with the theory of Tchen & Hinze [15], [16] as well as its extension by Deutsch [17], [18]

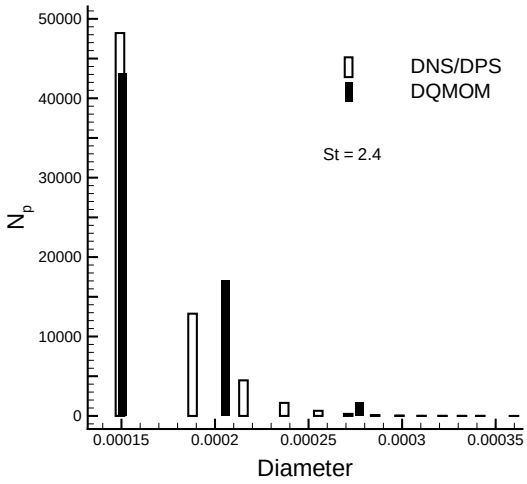

Figure 2. Particle number - diameter pdf for $St = 2.4$ at $Re_L = 61$

Table 1. Characteristics of fluid turbulence for turbulent Reynolds number $Re_L = 61.2$

Cube length	L_b	0.128
Grid points	N	128^3
Turbulent energy	q_f^2	$6.6616\,10^{-3}$
Integral longitudinal length scale	L_f/L_b	0.1056
Integral transversal length scale	L_g/L_f	0.4673
Reynolds number	Re_L	61.2
Kolmogorov length scale	η_k/L_b	0.0506
	$k_{max}\eta$	2.00

Table 2. DNS/DPS to DQMOM ratio of $0th$ to $5th$ order moment for particle inertia of $St = 0.1$, $St = 0.95$ and $St = 2.4$ at $Re_L = 61$ for simulation **case i**

moment (order)	$St = 0.1$	$St = 0.95$	$St = 2.4$
$N_p\ (0)$	2.004	1.238	1.102
$m_p\ (1)$	0.9994	1.0000	0.9995
$d_p\ (\frac{1}{3})$	1.669	1.168	1.073
$d_p^2\ (\frac{2}{3})$	1.323	1.087	1.039
(2)	0.353	0.750	0.877
(3)	0.138	0.620	0.920
(4)	0.113	0.789	2.191
(5)	0.212	1.857	11.114

Description of fluid-particle flow field

The fluid flow field is a homogeneous isotropic turbulence. Once the fluid flow field reaches a steady state the particulate phase is initiated and converges around an equilibrium with the fluid turbulence, as seen in figure 1. The particle Stokes numbers are chosen to be identical for different Reynolds numbers. The initial particle diameter d_p is the same in all simulations, only the particle density ρ_p is modified for different particle inertia. Table 1 summarizes the fluid field values for the turbulent Reynolds number $Re_L = 61$.

RESULTS

The results obtained from DNS/DPS simulations are compared with the DQMOM simulations described above under i) to v) in this section.

Case i)

DQMOM simulations are conducted for five different particle classes, as they are presented in figure 1. However, results are here only presented for the lowest, highest and the intermediate Stokes number. They are characterized by different particle inertia. As the DQMOM approach assumes 'molecular chaos' and thus independence of the coalescing particle velocities, it is supposed to perform best for high inertia particles, as this case is the closest to the 'molecular chaos' assumption. The DNS/DPS simulations are initialized with a monodisperse particle phase (all

particles have the same initial diameter), thus the particle size pdf is represented by one single Dirac function. As three Dirac functions are used in DQMOM to represent the particle diameter distribution, numerical problems could be caused by the initial monodisperse distribution. In order to avoid these problems, the DQMOM simulations are initialized with DNS/DPS data, in which three different particle sizes have occurred since the start of the coalescence simulation. As the DQMOM approach is written to conserve the first $2N-1$ moments of the particle diameter distribution, these moments are calculated for results obtained with the DNS/DPS as well as for results of the DQMOM (11). The ratio of the same moments of the corresponding distributions is used to evaluate the accuracy of the DQMOM in the here used configuration. Results are shown in table 2. Figure 2 compares distributions of inertial particles. The empty bars represent the Dirac distribution obtained from DNS/DPS simulations. As the initial distribution is monodisperse, all emerging droplet diameters are determined by the initial diameter. The black bars represent the Diracs from DQMOM.

Throughout this work, three Diracs are used in the DQMOM approach for two reasons. First, it appears the most feasible choice for comparison with the DNS/DPS data and second, the low-order moments give the same results for three or four Diracs as seen in table 3. Only the 4th-order and higher moments exhibit a significant change in magnitude. The choice of three Diracs seems to be justified. Naturally, if higher than 5th-order moments are of interest, an adequate number of Diracs needs to be chosen.

Under the impression of an increasing accuracy of the moments ratio DNS/DPS to DQMOM with increasing particle inertia, a dry granular test case was performed. Dry granular flows are performed for example in [1]. No fluid phase exists. The collision operator in DQMOM is based, as mentioned above, on the molecular chaos assumption. In dry granular flows this assumption leads to correct collisions frequencies, if the particles size distribution is correctly represented. If only binary collisions are treated and if the particle agitation per particle class is known and if one class exists for every different particle mass as well as for every emerging new particle mass, this approach should lead to correct collision frequencies for dry granular flows. In DQMOM, however, the number of particle classes (Diracs) is given and limited and thus compromises the results. Table 3 shows the moment ratios for this dry granular test case. In comparison with results for simulations with particle inertia of $St = 2.4$, the moment ratios of the dry granular test case exhibit an improvement of up to 50% error. Under the in case i) given conditions, the dry granular case can be considered as the most accurate result possible.

Table 3. DNS/DPS to DQMOM ratio of $0th$ to $5th$ order moment for particle inertia of $St = 2.4$ at $Re_L = 61$ with 3 respectively 4 Diracs and for the dry granular test case

moment (order)	dry granular q_p^2 DNS	$St = 2.4$ 3 Diracs	$St = 2.4$ 4 Diracs
N_p (0)	1.050	1.102	1.101
m_p (1)	1.0004	0.9995	0.9994
d_p $(\frac{1}{3})$	1.035	1.073	1.072
d_p^2 $(\frac{2}{3})$	1.019	1.039	1.038
(2)	0.947	0.877	0.878
(3)	0.972	0.920	0.917
(4)	1.475	2.191	2.101
(5)	4.320	11.114	9.515

Table 4. DNS/DPS to DQMOM ratio of $0th$ to $5th$ order moment for particle inertia of $St = 0.1$, $St = 0.95$ and $St = 2.4$ at $Re_L = 61$ for simulation **case ii**

moment (order)	$St = 0.1$	$St = 0.95$	$St = 2.4$
N_p (0)	1.876	1.220	1.121
m_p (1)	0.9994	1.0004	0.9995
d_p $(\frac{1}{3})$	1.589	1.155	1.086
d_p^2 $(\frac{2}{3})$	1.289	1.081	1.045
(2)	0.388	0.770	0.862
(3)	0.166	0.655	0.897
(4)	0.147	0.857	2.136
(5)	0.297	2.071	10.868

Case ii)

Results from additionally solving the particle kinetic stress equation using the theory of Tchen and Hinze [15] for the fluid particle covariance are presented in table 4. Results are similar for all particle inertia to those obtained under conditions given in i). Resolving the set of equations in ii) is applicable to less academic simulations as the here presented, in contrast to conditions under i).

Case iii)

Solving the fluid particle covariance equation in addition leads to results, presented in table 5, which show slightly worse

Table 5. DNS/DPS to DQMOM ratio of $0th$ to $5th$ order moment for particle inertia of $St = 0.1$, $St = 0.95$ and $St = 2.4$ at $Re_L = 61$ for simulation **case iii**

moment (order)	$St = 0.1$	$St = 0.95$	$St = 2.4$
N_p (0)	2.150	1.294	1.136
m_p (1)	0.9994	1.0004	0.9995
d_p $(\frac{1}{3})$	1.683	1.186	1.089
d_p^2 $(\frac{2}{3})$	1.300	1.086	1.043
(2)	0.489	0.862	0.927
(3)	0.345	0.965	1.162
(4)	0.552	1.760	3.595
(5)	1.990	5.925	24.306

Table 6. DNS/DPS to DQMOM ratio of $0th$ to $5th$ order moment for particle inertia of $St = 0.1$, $St = 0.95$ and $St = 2.4$ at $Re_L = 61$ for simulation **case iv**

moment (order)	$St = 0.1$	$St = 0.95$	$St = 2.4$
N_p (0)	2.173	1.310	1.148
m_p (1)	0.9994	1.0004	0.9995
d_p $(\frac{1}{3})$	1.700	1.202	1.103
d_p^2 $(\frac{2}{3})$	1.308	1.098	1.054
(2)	0.471	0.794	0.843
(3)	0.312	0.763	0.855
(4)	0.462	1.151	1.974
(5)	1.534	3.184	9.668

results as in the previous cases. Especially for the most interesting lowest order moments.

Case iv)

In this case, the collision term in the particle kinetic stress equation is added to the source terms. Results are shown in table 6. Comparison of results from case iii) and iv) shows a very similar performance. Only for the highest order moments results are better applying the collision term in the particle kinetic stress equation.

Case v)

Finally, in order to evaluate the influence of the collision term in the particle kinetic stress equation, simulations are done with and without this collision term in dry granular flows. The advantage of dry granular flows is the independence of the fluid properties and thus allows to evaluate the influence of this collision term in an isolated manner. It is the only remaining source term in the particle kinetic stress equation. Table 7 compares dry granular simulation results for three different simulations. First, resolving only the number and mass balance equation, while obtaining the particle kinetic energy in regular intervals from DNS/DPS simulations. Second, for two simulations solving the particle kinetic stress equation with and without collision term, respectively. In the first case, where the particle kinetic energy is obtained from the DNS/DPS data, an error of 5% remains for example for the particle number. This flow configuration is entirely controlled by the coalescence rate and thus the collision frequency, which requires a correct value for the particle kinetic energy per Dirac. As the update is done at fixed intervals, the collision frequency is calculated with not exact values for the particle kinetic energy.

Table 7. DNS/DPS to DQMOM ratio of $0th$ to $5th$ order moment for dry granular flows comparing results with different collision terms **case v**

moment (order)	$\mathcal{C}(\mu^k_{p,\alpha})$ q_p^2 DNS	$\mathcal{C}(\mu^k_{p,\alpha})$	$\mathcal{C}(\mu^k_{p,\alpha})$ $\mathcal{C}(c_{p,\beta}c_{p,\gamma}\mu^k_{p,\alpha})$
N_p (0)	1.050	1.063	1.009
m_p (1)	1.0004	1.005	1.005
d_p $(\frac{1}{3})$	1.035	1.043	1.014
d_p^2 $(\frac{2}{3})$	1.019	1.023	1.013
(2)	0.947	0.981	0.915
(3)	0.972	1.086	0.816
(4)	1.475	1.866	1.058
(5)	4.320	6.605	2.825

Introducing the particle kinetic stress equation provides an up-to-date value of the particle kinetic energy at each time increment. As can be seen in table 7 in the second column, results, however, did not improve. They exhibit even a slightly worse performance. Considering finally, as seen in the third column of table 7, a collision term in the particle kinetic stress equation, leads to a significant improvement of the results. For example, the particle number deviates less than 1% from the value obtained in dry DPS simulations. All other moments are in a good agreement either.

CONCLUSION

A recently developed extension of the DQMOM approach [2] based on the formalism of the joint fluid-particle PDF approach by Simonin [4] is evaluated. The great advantage of this extension is the possibility to write the particle momentum and particle kinetic stress transport equation accounting for coalescence effects. In particular a collision term in the particle kinetic stress transport equation can be written for the here presented case of Homogeneous Isotropic Turbulence. Several different cases, considering different sets of transports equations and collision terms (assuming molecular chaos) are compared to results obtained from DNS/DPS simulations. Their influence is evaluated and the overall performance of DQMOM is estimated. In dry granular flows an accuracy of less than 1% error in the particle number is obtained for DQMOM taking into account the collision term in the particle kinetic stress transport equation. As a correct prediction of the particle kinetic energy seems to be crucial to a good performance, other collision models will be tested in the future that take into account the fluid-particle interaction. In the here presented results the collision frequency in DQMOM is overestimated, thus the introduction of collision models that diminish the collision frequency like the correlated collision model in [9] could lead to an improved performance.

ACKNOWLEDGMENTS

Numerical simulations were performed on the NEC-SX8 supercomputer at the Institut de Développement et des Ressources en Informatique Scientifique (IDRIS). The CPU time has been provided by IDRIS in the frame of project 91066.

Financial support of Agence National de Recherche under project DYNAA is gratefully acknowledged.

This research project has been supported by a Marie Curie Early Stage Training Fellowship of the European Community's Sixth Framework Programme under contract number 'MEST-CT-2005-020429'.

REFERENCES

[1] Wunsch, D., Fede, P., and Simonin, O., 2008. "Development and validation of a binary collision detection algorithm for a polydispersed particle mixture". *Proceedings of the ASME FEDSM 2008,* **FEDSM2008-55159**.

[2] Belt, R. J., and Simonin, O., 2009. "Quadrature method of moments for the pdf modeling of droplet coalescence in turbulent two-phase flows". *Proceedings of the ASME FEDSM 2009,* **FEDSM2009-78095**.

[3] Marchisio, D. L., and Fox, R. O., 2005. "Solution of population balance equations using the direct quadrature method of moments". *Aerosol Sci.,* **36**, pp. 43–95.

[4] Simonin, O., 2000. "Statistical and continuum modeling of turbulent reactive particulate flows". *Von Karman Institute Lecture Notes*.

[5] Ashgriz, N., and Poo, J. Y., 1990. "Coalescence and separation in binary collisions of liquid drops". *J. Fluid Mech.,* **221**, pp. 183–204.

[6] Qian, J., and Law, C. K., 1997. "Regimes of coalescence and separation in droplet collision". *J. Fluid Mech.,* **331**, pp. 59–80.

[7] Estrade, J. P., 1998. "Etude expérimentale et numerique de la collision de gouttelettes". *Ecole nationale supérieure de l'aéronautique et de l'espace: Thèse*.

[8] Fevrier, P., Simonin, O., and Squires, K. D., 2005. "Partitioning of particle velocities in gas-solid turbulent flows into a continuous field and a spatially uncorrelated random distribution: theoretical formalism and numerical study". *J. Fluid Mech.,* **533**, pp. 1–46.

[9] Lavieville, J., Deutsch, E., and Simonin, O., 1995. "Large eddy simulation of interaction between colliding particles and a homogeneous isotropic turbulence field". *6^{th} Int. Symp. on Gas-Solid Flows, FEDSM 1995,* **228**, pp. 347–357.

[10] Fede, P., and Simonin, O., 2003. "Modelling of kinetic energy transfer by collision in a non-settling binary mixture of particles suspended in a turbulent homogeneous isotropic flow". *Proceedings of the ASME FEDSM 2003*.

[11] Simonin, O., Fevrier, P., and Lavieville, J., 2002. "On the spatial distribution of heavy-particle velocities in turbulent flow: from continious field to particulate chaos". *Journal of Turbulence,* **3, 040**.

[12] Eswaran, V., and Pope, S. B., 1988. "An examination of forcing in direct numerical simulations of turbulence". *Computers and Fluids,* **16 (3)**, pp. 257–278.

[13] Maxey, B. ., 1988. "Methods for evaluating fluid velocities in spectral simulations of turbulence". *Journal of Computational Physics,* **83**, pp. 96–125.

[14] Schiller, L., and Naumann, A., 1935. "A drag coefficient correlation". *VDI Zeitung,* **77**, pp. 318–320.

[15] Tchen, C. M., 1947. "Mean value and correlation problems connected with the motion of small particles suspended in a turbulent fluid". *Thesis: Delft, Martinus Nijhoff, The Hague*.

[16] Hinze, J. O., 1975. "Turbulence". *McGraw-Hill*.

[17] Deutsch, E., and Simonin, O., 1991. "Large eddy simulation applied to the motion of particles in stationary homogeneous fluid turbulence". *Turbulence Modification in Multiphase Flows,* **ASME FED, Vol. 110**, pp. 35–42.

[18] Sawford, B. L., 1991. "Reynolds number effects in lagrangian stochastic models of turbulent dispersion". *Phys. of Fluids,* **3 (6)**, pp. 1577–1586.